Chiral Molecules with Achiral Excited States: A Computational Study of 1,3-Dimethylallene

Eugen Deretey, Moshe Shapiro,* and Paul Brumer

Chemical Physics Theory Group, Department of Chemistry, University of Toronto, Toronto M5S 3H6, Canada

Received: February 13, 2001; In Final Form: July 5, 2001

Molecular orbital computations using the configuration interaction singles method and complete active space self-consistent field method were used to map out the electronic ground and excited states of 1,3-dimethylallene. Both open-shell and closed-shell singlet configurations were taken into account. Potential Energy Surfaces (PES) for the ground and the first two excited states were obtained over a two-mode grid composed of the C−C−C bending angle and the dihedral angle between the planes defined by the carbon atoms of the $H_3C-C=C$ and $C=C-CH_3$ groups. Several critical points located on the ground and first-excited PES were fully optimized by allowing all degrees of freedom to relax. The ground-state racemization reaction from the left-handed enantiomer to the right-handed was found to proceed via a barrier of 41 kcal/mol, in excellent agreement with the experimental value of 45.1 kcal/mol for the enthalpy of racemization. The ground-state transition-state geometry is shown to be planar-bent. The results indicate that 1,3-dimethylallene shows chiral structures in the ground state and achiral structures in the first-excited state. Coupled with the reported dipole-moment function, 1,3-dimethylallene is shown to be a useful molecule for coherently controlled racemic purification using our "laser distillation" scheme.

I. Introduction

There has been a great deal of interest recently[1−5] in the interaction of chiral molecules or racemic mixtures with coherent light. This includes, for example, efforts to understand the nature of coherent superpositions of chiral molecules,[1] as well as work such as ours on coherently controlled asymmetric synthesis using linearly polarized light.[3] A process that we term "laser distillation." Many of these studies share the common feature that the molecules are assumed to have a ground- state potential which supports chiral structures and an electronically-excited state which is achiral. Despite the interest in such molecules, however, there has been no systematic effort to identify molecules displaying these characteristics.

In this paper we show that 1,3-dimethylallene is a molecule of this type. 1,3-dimethylallene, a chiral molecule by virtue of the perpendicular positioning of the two methyl groups, was initially chosen for consideration because of its unique geometry. This allows the interconversion between the D and L enantiomers by simply breaking either of the double bonds, followed by a 180° rotation about that bond (see Figure 1). This suggests, as confirmed below, that although the breaking of a double bond is expected to be prohibited energetically on the ground state, it may well be facile on some of the excited states. Subsequent work, reported elsewhere,[6] showed that the structure of the potential surfaces, coupled with the dipole-moment function reported in this paper, allows for extensive chiral selectivity using our laser distillation scenario.[3]

To assess the utility of a molecule for laser distillation, or for the other studies cited above, required that we characterize all critical points. In the case of 1,3-dimethylallene there are a few studies of the spectra and internal rotation.[7,8] However, the many experimental[9−14] and computational[15−18] studies on the ground and excited states of allene, among them the computational study of the ring opening of substituted cyclopropylidenes to cyclic allenes,[16] suggest that computations must be done with care. Specifically, computational studies on the excited states of nonsubstituted allene are inconclusive regarding the character of local minima and other critical points on the first-excited-state surface. While Density Functional Theory (DFT) results in the first excited potential energy surfaces (PES) having a single minimum,[16] "Complete Active Space Multiconfiguration Self-Consistent Field" (CASSCF) based computations[17] suggest that the critical point at that geometry is a saddle point. For this reason we have initiated a careful and systematic exploration of the ground- and excited-state surface of 1,3-dimethylallene of all relevant critical points, characterizing their geometries and electronic configurations.

Section II below describes the methods of computation, followed by results for ground- and excited-state critical points and the dipole-moment function, in Section III.

II. Method of Calculation

The ground- and excited-state surfaces were computed over a rigid grid using single-excitation configuration interaction (CIS)[19,20] spanned by a double-ζ 6-31+G(d,p) basis set. In addition, full geometry optimizations of the critical points on the first excited PES of the planar 1,3-dimethylallene geometries were carried out using the CASSCF[21,22] with a triple-ζ 6-311+G(d,p) basis set. As the active CASSCF space, termed CASSCF(4,6), we have chosen four electrons and six orbitals. In the C_s planar configurations we have chosen four $\mathbf{a}'$ and two $\mathbf{a}''$ molecular orbitals, whereas for C_{2v} geometries the active space includes a single $\mathbf{b_1}$, $\mathbf{b_2}$, and $\mathbf{a_2}$ orbital and three $\mathbf{a_1}$ orbitals. The active space for the C_{2h} geometries is composed of an $\mathbf{a_g}$, $\mathbf{b_g}$, $\mathbf{a_u}$ and three $\mathbf{b_u}$ orbitals.

* Corresponding author, permanent address: Chemical Physics Department, The Weizmann Institute of Science, Rehovot, 76100, Israel.

10.1021/jp010557g CCC: $20.00
Published on Web 09/26/2001

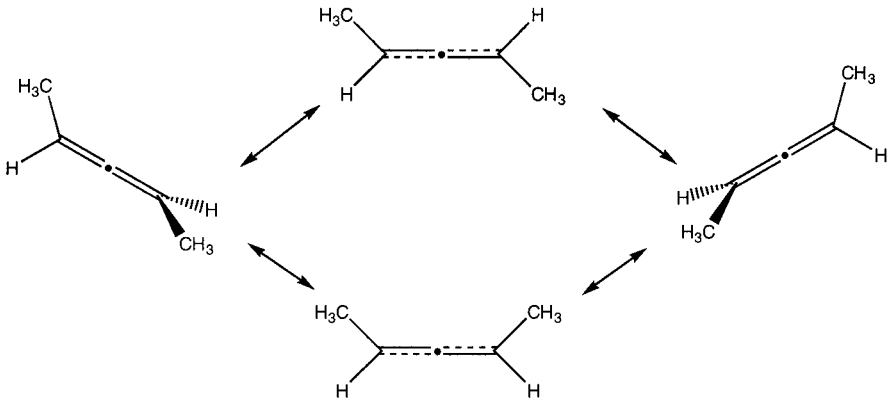

Figure 1. Racemization of 1,3-dimethylallene through internal rotation. The orthogonal left-handed enantiomer is converted to the right-handed enantiomer via the planar geometry.

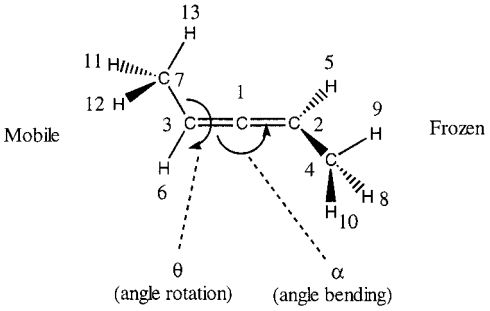

Figure 2. The geometry of the 1,3-dimethylallene used in the two-dimensional scan. The two variables in the rigid scan are (1) θ − the dihedral angle between the $H_3C-C=C$ and $C=C-CH_3$ planes; (2) α − the C−C−C bending angle, here shown by an arrow which brings the H_3C-C-H out of the plane of the paper.

All the calculations were carried out using the GAUSSIAN 94[23] program. The molecular orbital diagrams were generated by MOLDEN.[24]

III. Results

A. Two Variable PES for the Ground- and First-Excited States. The potential surfaces were computed on a grid as a function of two variables, α, the C−C−C bending angle, and θ, defined as the dihedral angle between the $H_3C-C=C$ and $C=C-CH_3$ planes (see Figure 2), for "in-plane" α and $\alpha = 0$, 180°, and as $\phi - 90°$ where ϕ is the dihedral angle between the H3C−C=C plane and the C=C=C plane for the out-of-plane bending angle $\alpha' \neq 0$, 180°.

For linear 1,3-dimethylallene θ is identical to the torsional angle $H_3C-C\cdots C-CH_3$. The range of θ explored was [0°, 180°], where (see Figure 1) 0° and 180° correspond to the two planar geometries and 90° − to one of the orthogonal 1,3-dimethylallene geometries. Because of symmetry we did not need to explore the 180° to 360° range.

As a result of the methyl substituents, there are three principal inequivalent bending directions of the linear C=C=C group (see Figure 3): (a) "In-plane" bending by angle α- confined to the frozen $H_3C-C=C$ plane. (b) "Out-of-plane" bending by angle α'- i.e., bending in a direction orthogonal to the frozen $H_3C-C=C$ plane. This bending will generate nonplanar geometries, which are precursors for ring closure to yield the cyclopropylidene.[16] (c) Bending at 45° between the above directions. Bending in this direction preserves the C_2 symmetry of 1,3-dimethylallene.

We have computed the potential energy surfaces for the bending motion in the (a) and (b) directions, where the bending angle was allowed to vary between 100°and 260°. Figure 4 shows the ground and the first two excited PES generated by the CIS method for the in-plane bending. Figure 5 shows the same data for the out-of-plane bending. Note that in both cases the ground state shows two wells with a barrier between them along $\theta = 180°$, corresponding to the two ground-state chiral species, whereas the first-excited state shows a well with a minimum at $\theta = \alpha = 180°$. This is precisely the PES structure one seeks for the chiral studies cited above-i.e. the ground state is chiral whereas the (first) excited state is not.

The geometries of the rigid scan critical points are shown in Figure 6 and Figure 7. In Figure 6 we display six critical geometries of the planar 1,3-dimethylallene molecule. Since the planar geometries at (θ,α)=(180°,120°), and (180°,240°) geometries are identical, there are five independent critical geometries. We note that the structure located at (360°,240°), for which the two methyl groups are very close to one another, is very unfavorable energetically.

In Figure 7 we display six critical geometries in the out-of-plane bending configurations of the first excited state. Only two of them, (θ,α') = (180°,180°) and (360°,180°) are of sufficient low energy to be of interest in this study. They are similar to

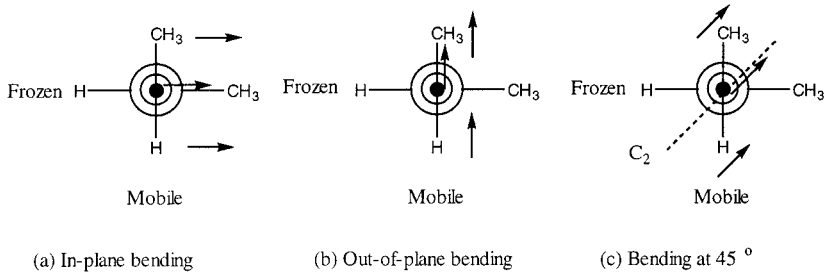

Figure 3. Three main modes of distortion for the 1,3-dimethylallene C=C=C group. The Newmann projection is shown along the C=C=C moiety. Arrows show the movement of the CH_3–C−H mobile group (the second C atom from the left is symbolized by a black dot).

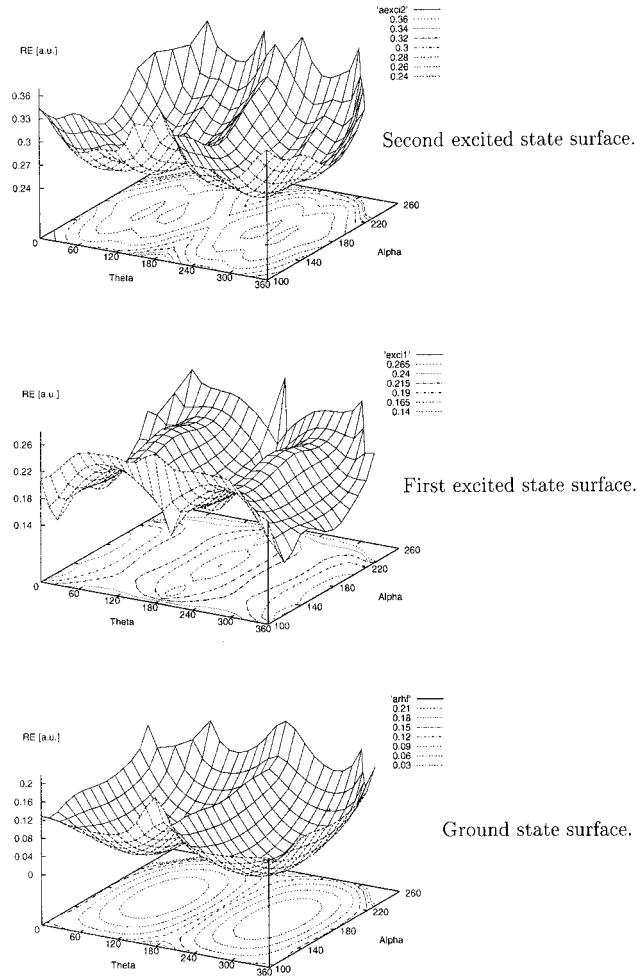

Figure 4. In-plane bending surfaces. α is the C−C−C bending angle and θ is the dihedral angle. The orthogonal linear 1,3-dimethylallene is the global ground-state minimum.

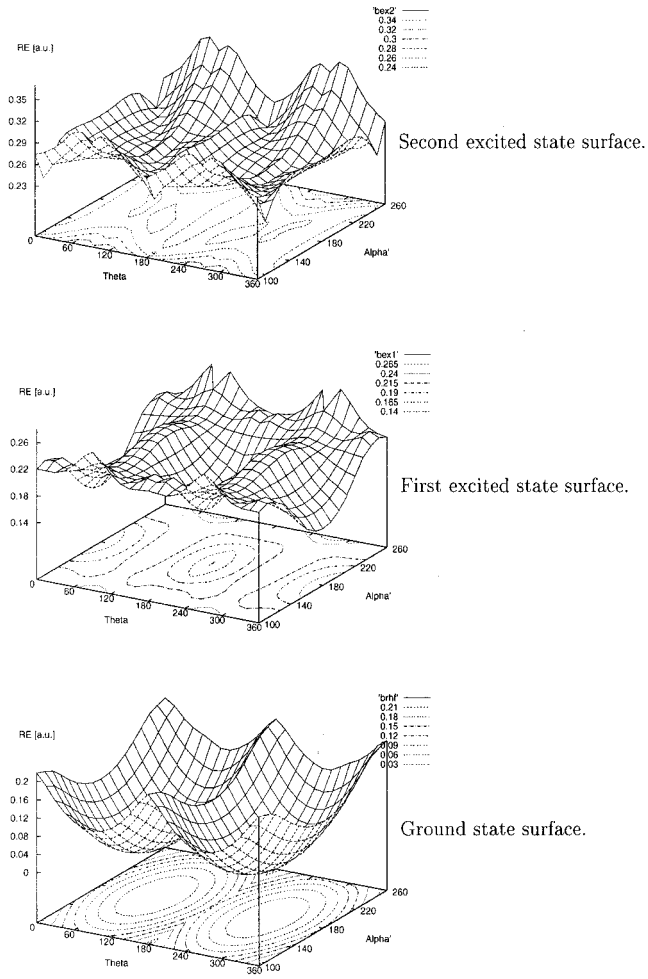

Figure 5. The same as in Figure 4 but for the out-of-plane bending surfaces. In this case the C−C−C bending angle is denoted **α'**.

TABLE 1: The CAS Coefficients of the Most Important Configuration[a]

State	*anti-* linear	*syn-* linear	*anti-* bent	*syn-* bent
Closed shell singlet (1,2)(1,2)	0.99926	0.99940	0.96199	0.96601
Open shell singlet (1,2)(1,3)	0.99998	0.99998	0.99999	0.99999
Open shell triplet (1,2,3)(1)	0.99998	0.99997	0.99999	0.99998

[a] Planar-linear geometries with a (1,2)(1,2) CAS coefficient bigger then 0.999 are considered to be "pure". In the planar-bent geometries, in addition to the dominant (1,2)(1,2) configuration, there is a small contribution from the doubly excited (2,3)(2,3) configuration.

the in-plane critical points. The other four geometries are precursors to the cyclopropylidene ring closure.

B. CASSCF Optimization at the Planar Critical Points. The limited scan over the two angles reported above only yields approximate locations for the critical points. To refine our understanding, we have performed, using CASSCF, full-dimensional optimization at the planar critical geometries uncovered by our two-dimensional search. These calculations were performed for both closed- and open-shell singlets and for one open-shell triplet state.

Figure 8 shows the six orbitals and the four electrons considered in the active space. The electronic configurations are identified by four numbers composed of the orbital number (1,2,...,6), with the first two numbers carrying an α spin and the last two numbers a β spin. For example, the notation (1,2)(1,2) implies that the first electron is assigned to orbital 1,

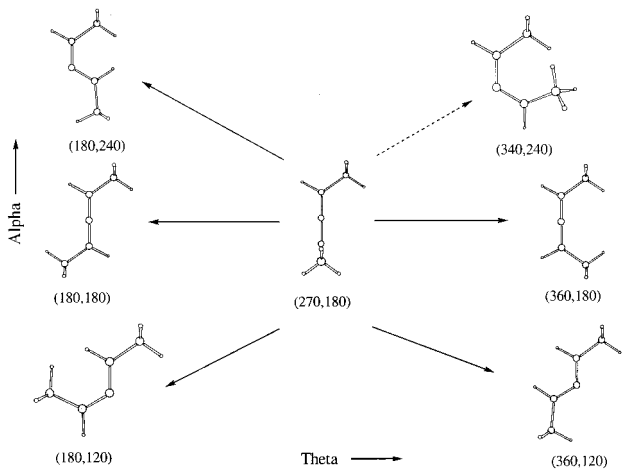

Figure 6. The geometries of some low energy critical points found by an "in-plane" rigid scan over the ground and first excited PES. Numbers below the figures denote values of (θ,α). Note that the figure in the center is on the ground electronic state and those on the outside are on the first excited electronic state.

the second electron to orbital 2, both with α spins; the third electron to orbital 1 and the fourth electron to orbital 2, both with β spins.

Save for some specific configurations, all the geometric parameters were relaxed in the optimization, with no symmetry constraints imposed. The resultant energies[25] and coefficients for the most important electronic states are given in Table 1

TABLE 2: CAS(4,6)/6-311+G(d,p) Energies for the Ground State and Excited State Planar 1,3-Dimethyl Allene[a]

Electronic state	*anti*-linear	*syn*-linear	*anti*-bent	*syn*-bent
		CAS energy [hartree]		
Closed shell singlet (1,2)(1,2)	−193.866194	−193.867627[c]	−193.909096	−193.920042
Open shell singlet (1,2)(1,3)	−193.908078	−193.907871	−193.922921	−193.921624
Open shell triplet (1,2,3)(1)	−193.911049	−193.910845	−193.926780	−193.925483
		CAS energy relative to the open shell singlet species [kcal/mol][b]		
Closed shell singlet (1,2)(1,2)	26.283 (76.439)[d]	25.253 (75.540)	8.675 (49.518)	0.993 (42.649)
Open shell singlet (1,2)(1,3)	0.000 (50.156)	0.000 (50.287)	0.000 (40.843)	0.000 (41.656)
Open shell triplet (1,2,3)(1)	−1.864 (48.293)	−1.866 (48.421)	−2.422 (38.421)	−2.422 (39.235)

[a] For ground state, orthogonal 1,3-dimethylallene $E_{CAS} = -193.988008$, $CAS_{coeff} = 0.99999$, C=C=C angle = 179.9°. [b] Numbers are given to three significant figures, as obtained in the calculation. No claim of such accuracy is of course claimed here. If judging by the agreement with the experimental[8] $\Delta H_{racemization} = 45.1$ kcal/mol value, than these numbers are only accurate to ±2−3 kcal/mol. [c] See ref 25. [d] Bracketed numbers are calculated with respect to the orthogonal 1,3-dimethylallene.

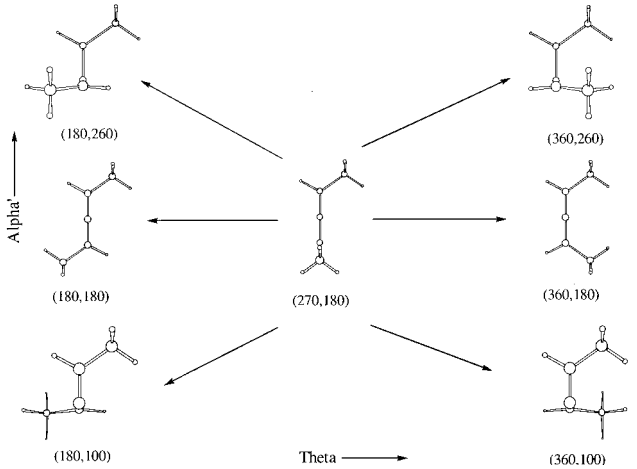

Figure 7. The same as in Figure 4 but for the "out-of-plane" scan. In this case the numbers below the figures denote values of (***θ***,**α'**).

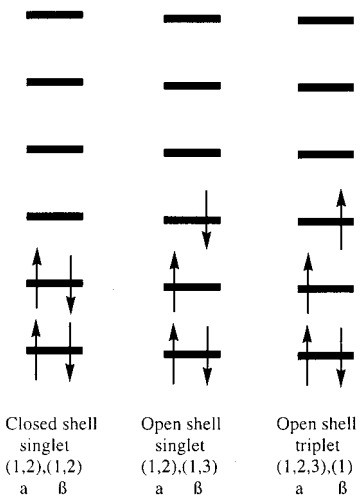

Figure 8. Examples of closed- and open-shell electronic configurations included in the active space in CAS(4,6) and their symbolic notation.

and Table 2. The calculated geometries, the atom serial numbers, the bond length, and bond angles are given in Figs. 2, 9, 10, Table 3, and Table 4. The highest occupied and lowest unoccupied molecular orbitals are shown in Figure 11.

It is instructive to follow the way in which the bending of the C−C−C angle affects the closed-shell planar energies. To do so, we performed single-point CASSCF calculations at the linear-anti and the slightly bent C−C−C geometries. The results are shown in Figure 12. Bending from 180° to ≈165° shows smooth energy variations on the excited- electronic state with closed-shell singlet configuration. Additional bending below

TABLE 3: Bond Lengths and Bending Angles for Linear and Planar-Bent Geometries[a]

Atom label	Linear *anti*			Linear *syn*		
	Bond length [Å]			Bond length [Å]		
	1a	**1b**	**1c**	**2a**	**2b**	**2c**
2,1	1.318	1.344	1.343	1.318	1.344	1.343
3,1	1.318	1.344	1.343	1.318	1.344	1.343
4,2	1.517	1.507	1.507	1.518	1.508	1.508
5,2	1.079	1.083	1.083	1.078	1.083	1.083
6,3	1.079	1.083	1.083	1.078	1.083	1.083
7,3	1.517	1.507	1.507	1.518	1.508	1.508
8,4	1.086	1.088	1.088	1.086	1.088	1.088
9,4	1.085	1.083	1.083	1.085	1.084	1.084
10,4	1.086	1.088	1.088	1.086	1.088	1.088
11,7	1.086	1.088	1.088	1.086	1.088	1.088
12,7	1.086	1.088	1.088	1.086	1.088	1.088
13,7	1.085	1.083	1.083	1.085	1.084	1.084
	Bending angle [degrees]			Bending angle [degrees]		
3,1,2	180.000	180.000	180.000	179.634	180.000[b]	180.000[b]
4,2,1	123.822	124.881	124.952	123.410	125.031	125.107
5,2,1	114.285	119.123	119.114	114.852	118.978	118.965
6,3,1	114.285	119.123	119.114	114.852	118.978	118.965
7,3,1	123.822	124.881	124.952	123.410	125.031	125.107
8,4,2	111.281	110.608	110.611	111.257	110.808	110.809
9,4,2	111.065	111.480	111.476	111.241	111.136	111.138
10,4,2	111.281	110.608	110.611	111.257	110.808	110.809
11,7,3	111.281	110.608	110.611	111.257	110.808	110.809
12,7,3	111.281	110.608	110.611	111.257	110.808	110.809
13,7,3	111.065	111.480	111.476	111.241	111.136	111.138

[a] The triplet open shell geometries, **1c** and **2c**, were included for comparative purposes. [b] The C−C−C bending angle together with four dihedral angles were frozen during the optimization.

≈165° leads to the sudden "collapse" of the CASSCF calculation to the lower-energy, open-shell, ground-state configuration. At bending angles of 130° and below, the stable excited-state CASSCF configuration again returns to a closed-shell excited state.

Figure 12 shows the presence of a near crossing between the open-shell (1,2)(1,2) singlet and the closed-shell (1,2)(1,3) singlet at ≈165°. The existence of an "avoided crossing" is further confirmed by the interchange of the HOMO−LUMO orbitals in linear and bent geometries as seen in Figure 11. It is conceivable that the "collapse" of the CASSCF calculation noted above results from the failure of the Born−Oppenheimer approximation in this near crossing region. In the present study we did not try to locate the crossing point more accurately because our main purpose was to study the planar structures, further details about which are given in section IV.

C. The Electric Dipole-Moment for the Ground and the First Excited States. Studies of light-induced processes in chiral molecules, the motivation for this study, require the electric-dipole moment as input into the computation of Franck−Condon

TABLE 4: Bond Lengths and Bending Angles for Planar-bent Geometries[a]

Atom label	Bent *anti*			Bent *syn*		
	Bond lengths [Å]			Bond lengths [Å]		
	3a	**3b**	**3c**	**4a**	**4b**	**4c**
2,1	1.399	1.413	1.413	1.392	1.357	1.357
3,1	1.392	1.321	1.321	1.392	1.357	1.357
4,2	1.506	1.503	1.503	1.492	1.500	1.500
5,2	1.083	1.075	1.075	1.091	1.082	1.082
6,3	1.087	1.083	1.083	1.091	1.082	1.082
7,3	1.493	1.504	1.504	1.492	1.500	1.500
8,4	1.088	1.088	1.088	1.089	1.088	1.088
9,4	1.080	1.083	1.083	1.081	1.084	1.084
10,4	1.088	1.088	1.088	1.089	1.088	1.088
11,7	1.089	1.088	1.088	1.089	1.088	1.088
12,7	1.089	1.088	1.088	1.089	1.088	1.088
13,7	1.081	1.084	1.084	1.081	1.084	1.084
	Bond angles [degree]			Bond angles [degree]		
3,1,2	113.442	139.161	138.763	108.746	137.530	137.202
4,2,1	133.243	123.932	124.103	124.461	124.704	124.737
5,2,1	115.738	118.000	117.927	121.364	117.772	117.806
6,3,1	123.571	118.606	118.638	121.364	117.772	117.806
7,3,1	123.134	124.917	124.850	124.461	124.704	124.737
8,4,2	108.722	110.764	110.764	109.826	110.929	110.905
9,4,2	115.292	111.948	111.968	111.048	111.211	111.219
10,4,2	108.722	110.764	110.764	109.826	110.929	110.905
11,7,3	109.845	110.779	110.780	109.826	110.929	110.905
12,7,3	109.845	110.779	110.780	109.826	110.929	110.905
13,7,3	110.967	111.178	111.188	111.048	111.211	111.219

[a] The triplet open shell geometries, **3c** and **4c**, were included for comparison.

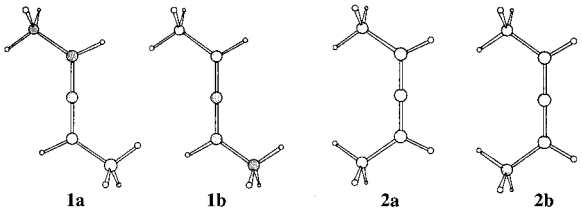

Figure 9. Calculated planar-linear geometries. The **1a**, **2a** geometries have closed shell configurations. The **1b**, **2b** geometries have open shell configurations.

factors. Computational results on the electric-dipole are provided in this section.

We have computed the electric-dipole moment for the ground state and first- electronic-excited state of 1,3-dimethylallene using the same procedure as for the potential energy surfaces. The *X*, *Y* and *Z* components (see note[26]) of the dipole in ground- and excited-electronic states are shown in Figures 13 and 14 for fixed **α,** and as a function of θ. We found that for the linear orthogonal-conformation $(\theta,\alpha) = (90, 180)$, the dipole-moment of the first-excited state is four-times larger than that of the ground state. In contrast, the dipole moment for the planar anti-conformation $(\theta,\alpha) = (180, 180)$ is essentially zero in both ground- and first-excited states, and remaining linear-planar conformations show a generally small dipole in both the ground and excited states. The dipole functions for the bent conformations are somewhat more complicated. The total electric-dipole moment surfaces for the ground state and first-electronic-excited state are shown in Figure 15.

IV. Optimized Configurations and Racemization

In this section we discuss the results of fully optimized studies, carried out at select geometries using the CASSCF method, as well as the energetics of the 1,3-dimethylallene racemization reaction.

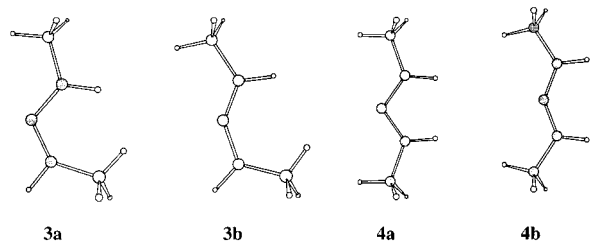

Figure 10. Calculated planar-bent geometries. The **3a**, **4a** geometries have closed shell configurations. The **3b**, **4b** geometries have open shell configurations.

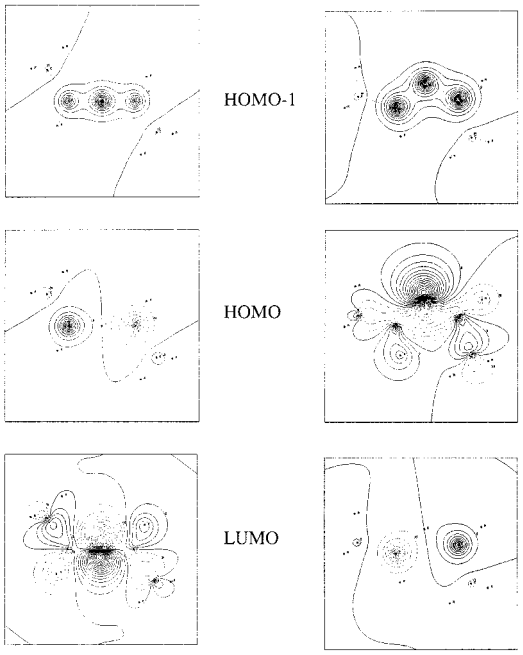

Figure 11. Molecular orbitals of the planar-linear C_{2h} and planar-bent C_{2v} symmetries.

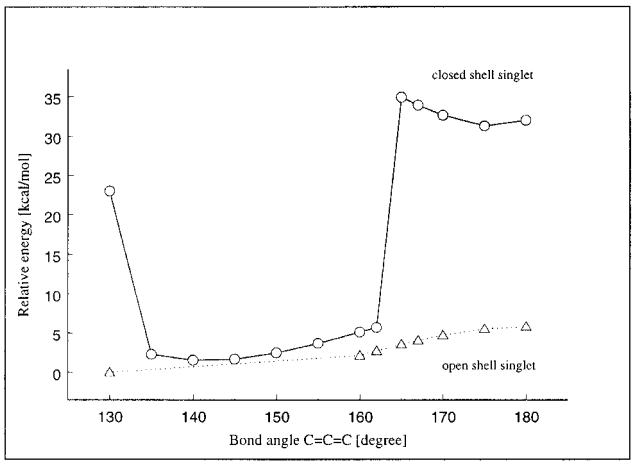

Figure 12. The energy of planar-anti 1,3-dimethylallene as a function of the C−C−C bending.

From the viewpoint of electronic structure, our most important finding is that the ground PES is dominated by a closed-shell (1,2)(1,2) configuration in the orthogonal geometry and by an open-shell (1,2)(1,3) configuration in the planar geometries. The *reverse* occurs in the first-excited state: this state is dominated by the open-shell (1,2)(1,3) configurations in the orthogonal geometries and by a closed-shell configuration (1,2)(1,2) in the planar geometries. This alternation between open- and closed-shell configurations is similar to that found for allene.[16]

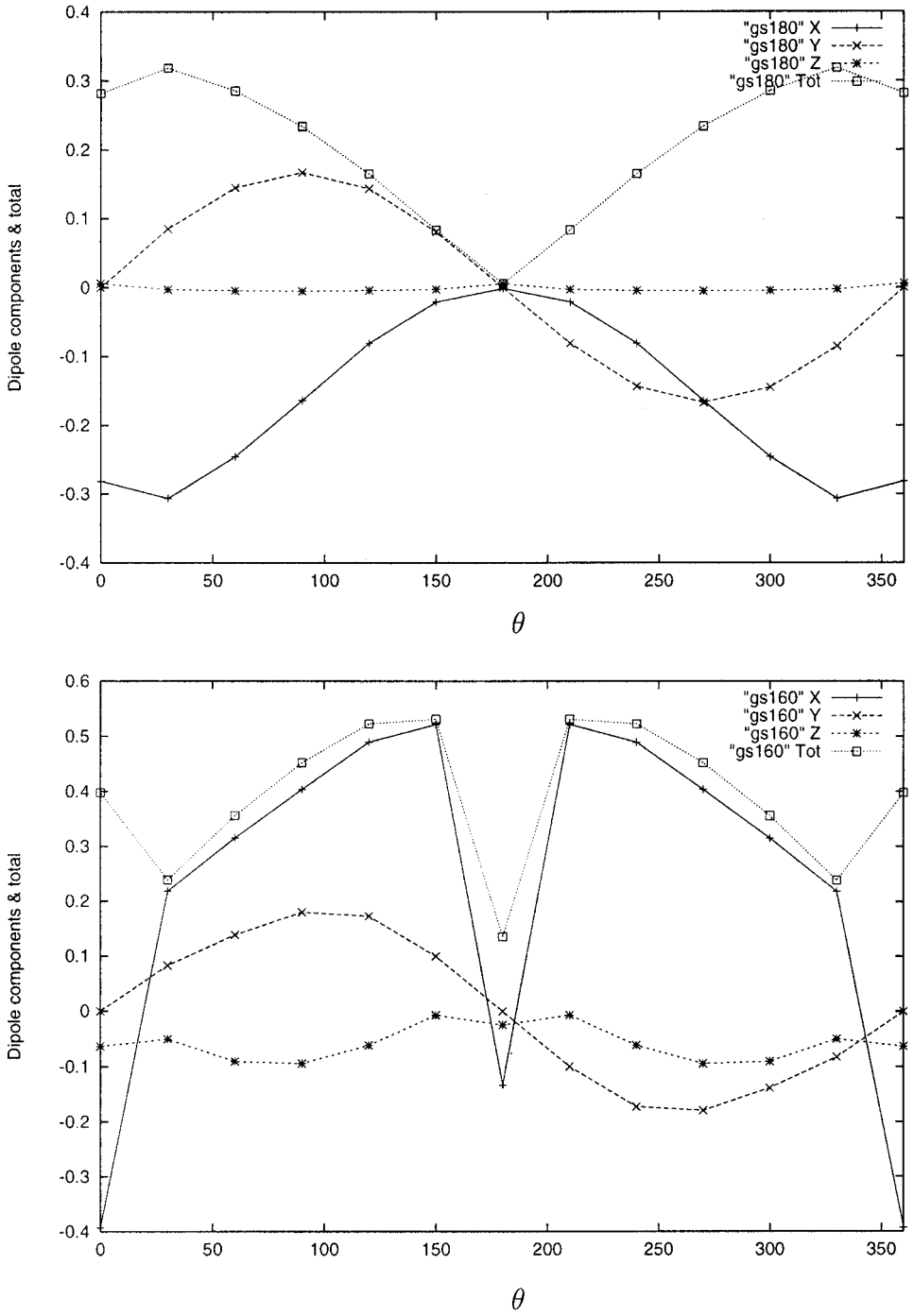

Figure 13. The ground-state electric-dipole moment as a function of θ for two values of α [$\alpha = 180$ for the linear configuration in the upper panel, and $\alpha = 160$ in a bent configuration in the lower panel]. Shown are the X (denoted by plus signs), Y (denoted by x's), and Z (stars) components of the electric dipole, as well as the total electric dipole moment (denoted by boxes).

We found that at the same geometry, the ground PES has a saddle point and the first-excited PES has a minimum. We identify the ground PES saddle point with the transition state for the interconversion of *L* 1,3-dimethylallene to *D* 1,3-dimethylallene. In addition, we find that, a) the first-excited surface minimum is characterized by a closed-shell configuration; b) at the geometry of the first-excited-state minimum the first excited state is higher in energy than the ground state; c) the ground PES saddle point, occurring at the same geometry, is dominated by an open-shell configuration.

A. Planar Geometries. *1. Planar-Linear Geometries.* At the planar-linear geometries the CASSCF coefficients show that the ground PES is almost entirely made up of the (1,2)(1,3) open-shell configuration, while the first-excited PES is dominated by the (1,2)(1,2) closed-shell configuration. We find that the energy difference between the open- and closed-shell planar-linear geometries is ≈26 kcal/mol. These findings are qualitatively similar to the situation in nonsubstituted allene, though for 1,3-dimethylallene the energy gap is higher.

In both electronic states there is no difference in energy between the anti- and syn-planar-linear geometries. Presumably the distance between the methyl groups is so large that there is essentially no interaction between these two groups at these geometries (see Table 3 and Ref 27).

2. Planar-Bent Geometries. At the planar-bent geometries the ground- and first-excited states have a similar electronic

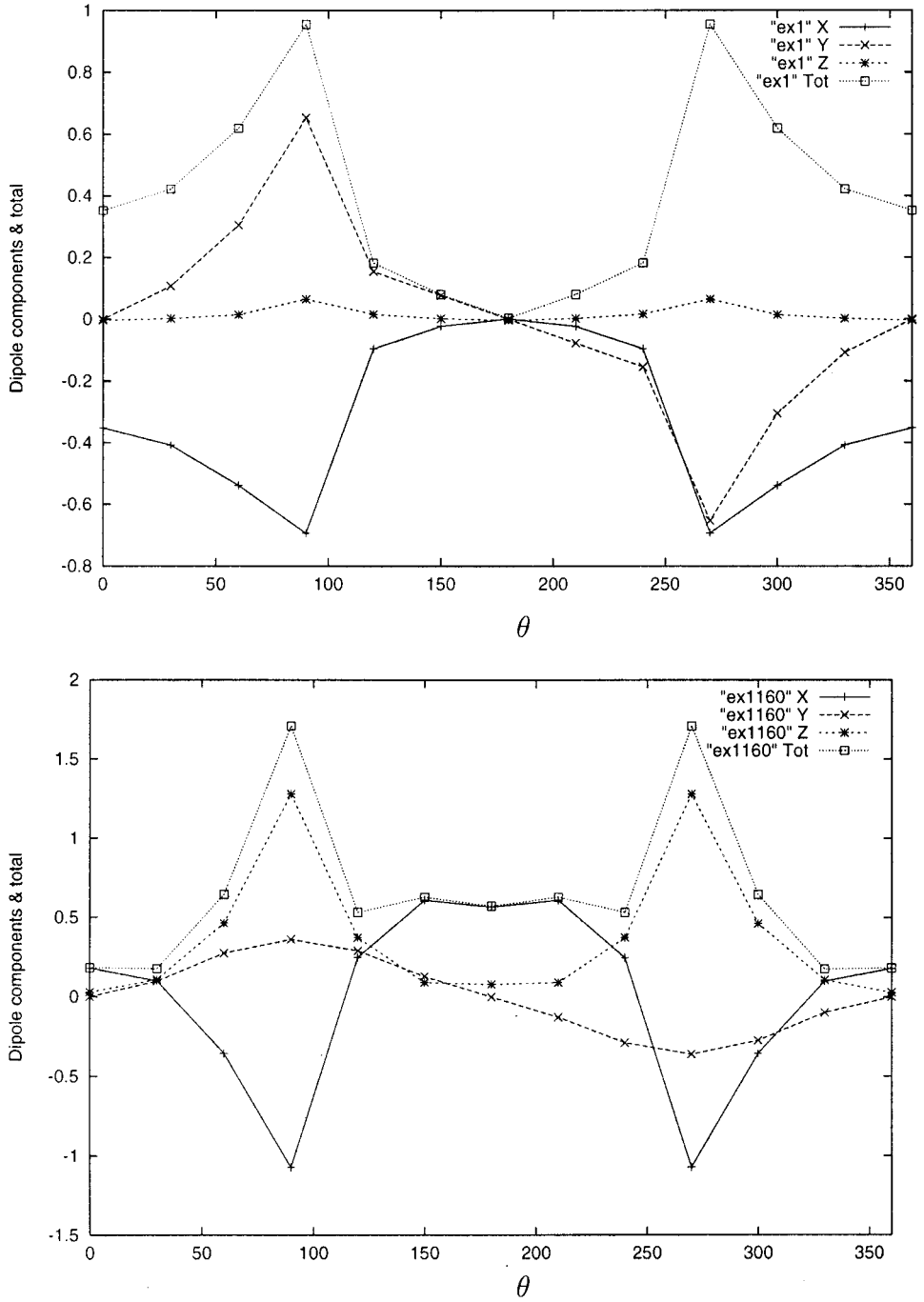

Figure 14. As in Figure 13, but for the first excited-state electric-dipole moment.

character to that of the planar-linear geometries, except for some mixing with the (2,3)(2,3) doubly-excited closed-shell configuration[28] (see Table 1).

Contrary to the situation in the planar-linear case, in the planar-bent case the energy difference between the ground− and first-excited state does depend on whether the system is in the anti or syn geometry: The energy difference is ≈8.6 kcal/mol for the planar-bent-anti geometries, and ≈1.0 kcal/mol for the planar-bent-syn geometries (see Table 2, Figure 9 and Figure 10), the syn being always lower in energy in the first-excited state. The energy difference between these two planar-bent geometries is ≈7 kcal/mol. By contrast, there is essentially no difference in energy between these geometries in the ground state.

The syn-anti-energy difference is a direct result of the C−C−C bending angle where the PES has a local minimum. In the first-excited state anti configuration this angle is 113°, whereas in the syn configuration it is 108°. Both values are much smaller than the C−C−C bending angle minimizing the ground PES, which is 139°in the anti configuration and 137.5°in the syn configuration (see Table 4). As a result, the methyl groups are much closer in the first-excited state[27] and interact more, thereby explaining the difference in energy between the syn and anti geometries in the first-excited state.

One of the most prominent features, observed in Table 3, to come out of our calculation is the shortening of the C−C bond-lengths in the first-excited state planar-linear geometry. The optimized geometries are displayed in Figure 9(1a) for the first-excited-state-C_{2h} symmetry and in Figure 9(**2a**) for the first-excited-state-C_s symmetry. The ground-state geometry having a C_{2h} symmetry is shown in Figure 9(**1b**), and that belonging to the C_{2v} symmetry is shown in Figure 9(**2b**). The shortening

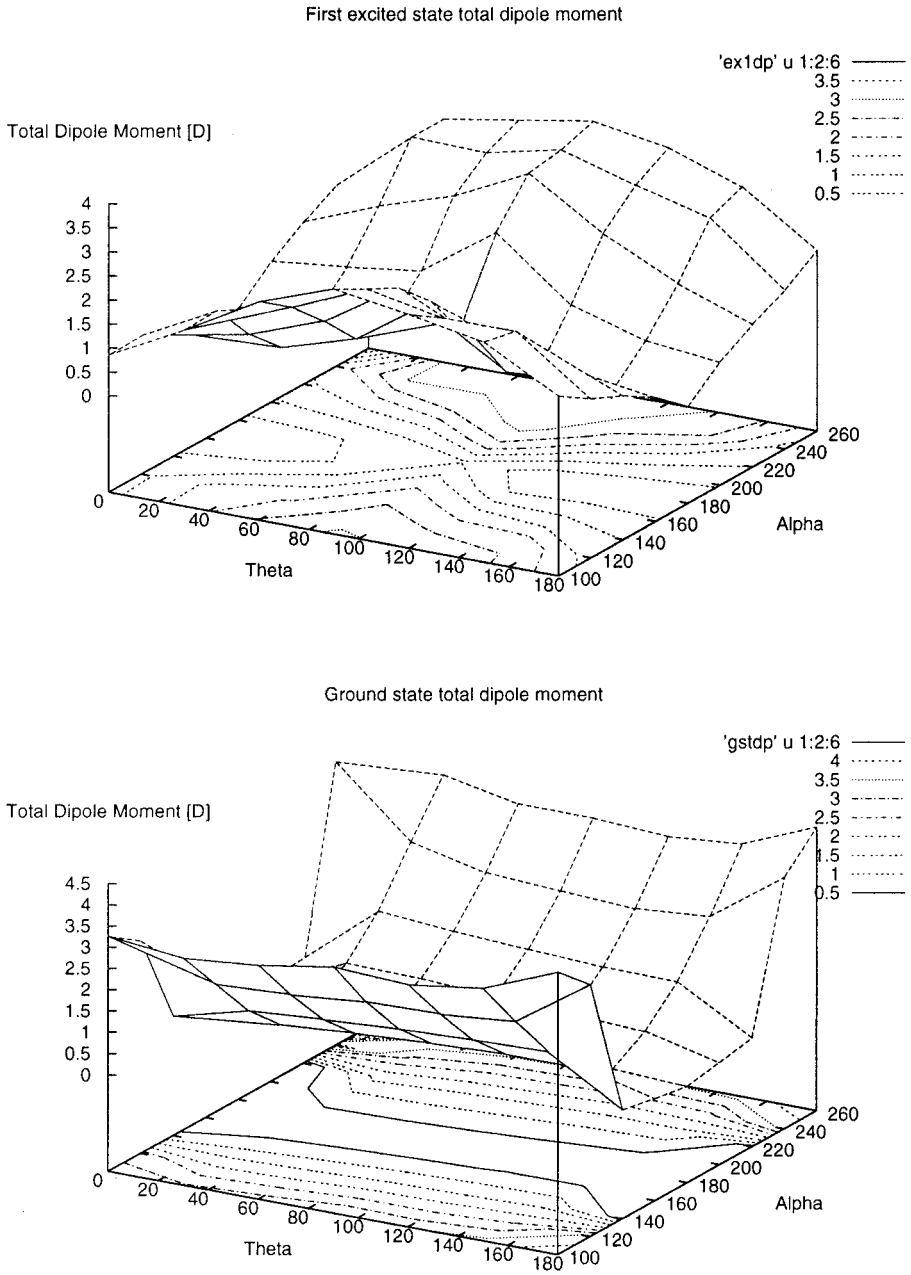

Figure 15. The electric-dipole moment as a function of θ and α − the dihedral and bending angles.

of the C−C bond length occurs for both the anti and the syn geometries.

The open-shell triplet-planar structures are about 2 kcal/mol lower in energy than the open-shell singlet structures. There is almost no difference between the open- shell-singlet and the open-shell-triplet geometries, as shown in Table 3.

B. The Racemization Reaction. To complete the calculation of the minimum-energy path for the racemization reaction, which is the transition from one orthogonal-linear geometry to its enantiomeric form, we have performed CASSCF optimization at the *orthogonal* geometry. At this geometry the ground-state was found to be composed essentially of a single closed-shell (1,2)(1,2) configuration. In contrast, the first-excited state was found to be composed of a number of open-shell configurations, with the (1,2)(1,3) configuration being most prominent.

Having performed the optimization for both the orthogonal-linear and planar geometries, the current calculation suggests that the racemization reaction proceeds via the planar-bent geometry. The transition-state energy-barrier at this geometry without any temperature correction was computed here to be 41 kcal/mol. This barrier height and the transition-state geometries are in good agreement with experimental findings.[8] In particular, the experimental value for the enthalpy of racemization was found to be 45.1 kcal/mol,[8] this is in excellent agreement with our computed energy barrier. In contrast, the path which proceeds via the planar-linear geometry is more costly in energy: it involves a barrier of 50 kcal/mol.

V. Conclusions

We computed the ground and first-excited-state PES of 1,3-dimethylallene as a function of the C−C−C bending angle and the dihedral angle between $H_3C-C=C$ and $C=C-CH_3$ planes at the CIS level. We also performed a full CASSCF optimization at a number of critical configurations in both the ground and first-excited PES.

We have shown that the ground-state racemization reaction from one enantiomeric form of 1,3-dimethylallene to the other

proceeds via a barrier of 41 kcal/mol, in excellent agreement with the experimental value of 45.1kcal/mol for the enthalpy of racemization. The ground-state transition state geometry was shown to be planar-bent.

We also found that the first excited PES possesses a stable low energy critical point at the planar-bent geometry corresponding to the ground-state transition state. Thus, this study suggests that 1,3-dimethylallene has a ground-state potential energy surface that supports chiral structures, and an excited electronic state that is achiral. Further, the minimum in the upper potential lies above the ground-state transition state from the Dextro to the Levo form. As a consequence 1,3-dimethylallene is a useful molecule for many of the proposed studies of coherent light interacting with a chiral species.[1−4] In particular, in a subsequent publication[6] we demonstrate the ability to "laser distill"[3] 1,3-dimethylallene so as to selectively produce a large enantiomeric excess using linearly polarized light and a polarized dimethylallene medium.

Acknowledgment. We thank Professor Malcolm Bersohn, University of Toronto, for his suggestion that we consider 1,3-dimethylallene as a candidate for laser distillation, and for subsequent discussions. This work was partially supported by a grant from the EU IHP IHP-RTN-99-1 Program and by the U.S. Office of Naval Research.

References and Notes

(1) Maierle, C. S.; Harris, R. A. *J. Chem. Phys.* **1998,** *109*, 3713; Cina, J. A.; Harris, R. A. *J. Chem. Phys.* **1994,** *100*, 2531.

(2) Quack, M. *Angew. Chem. Ed. Engl*. **1989,** *28*, 571.

(3) Shapiro, M.; Frishman, E.; Brumer, P. *Phys. Rev. Lett.* **2000**, *84*, 1669.

(4) Fujimura Y.; Gonzalez, L.; Hoki, K.; Manz, J.; Ohtsuki, Y. *Chem. Phys. Lett.* **1999,** *306*, 1.

(5) Salam A.; Meath, W. J. *J. Chem. Phys.* **1997,** *106*, 7865; Salam A.; Meath, W. J. *J. Chem. Phys.* **1998,** *228*, 115.

(6) D. Gerbasi, M. Shapiro and P. Brumer, (manuscript in preparation).

(7) Rauk, A.; Drake, A. F.; Mason, S. F. *J. Am. Chem. Soc*. **1979**, *101*, 2284.

(8) Roth, W. R.; Bastigkeit, T. *Liebigs Ann. Chem.* **1996**, 2171.

(9) Iverson, A. A.; Russel, B. R. *Spectrochim. Acta, Part A* **1972**, *28A*, 447.

(10) Fuke, K.; Schnepp, O. *Chem. Phys*. **1979**, *38*, 211.

(11) Baltzer, P.; Wannberg, B.; Lundqvist, M.; Karlsson, L.; Holland, D. M. P.; MacDonald, M. A.; von Niessen, W. *Chem. Phys*. **1995**, *196*, 551.

(12) Bawagan, A. D. O.; Ghanty, T. K.; Davidson, E. R.; Tan, K. H. *Chem. Phys. Lett.* **1998**, *287*, 61.

(13) Holland, D. M. P.; Shaw, D. A. *Chem. Phys.* **1999**, *243*, 333.

(14) Mahapatra, S.; Cederbaum, L. S.; Koppel, H. *J. Chem. Phys.* **1999**, *111*, 10452.

(15) Seeger, R.; Krishnan, R.; Pople, J. A.; Schleyer, P.V.R. *J. Am. Chem. Soc.* **1977**, *99*, 7103.

(16) Bettinger, H. F.; Schreiner, P. R.; Schleyer, P.V.R.; Schaefer, III, H. F. *J. Phys. Chem*. **1996**, *100*, 16147. Bettinger, H. F.; Schreiner, P. R.; Schleyer, P. v. R.; Schaefer, III, H. F. *J. Org. Chem*. **1997**, *62*, 9267.

(17) Jackson, W. M.; Mebel, A. M.; Lin, S. H.; Lee, Y. T. *J. Phys. Chem.* **1997**, *101*, 6638 and references wherein.

(18) Otto, P.; Ruiz, M. B. *J. Mol. Struct. (THEOCHEM)* **1998**, *433*, 131.

(19) Foresman, J. B.; Head-Gordon, M.; Pople, J. A.; Frisch, M. J. *J. Phys. Chem*. **1992**, *96*, 135.

(20) Stanton, J. F.; Gauss, J.; Ishikawa, N.; Head-Gordon, M. *J. Chem. Phys*. **1995**, *103*, 4160.

(21) Schlegel, H. B.; Robb, M. A. *Chem. Phys. Lett*. **1982**, *93*, 43.

(22) Bernardi, F.; Bottoni, A.; McDougall, J. J. W.; Robb, M. A.; Schlegel, H. B. *Faraday Symp. Chem. Soc*. **1984**, *19*, 137.

(23) Frisch, M. J.; Trucks, G. W.; Schlegel, H. B.; Gill, P. M. W.; Johnson, B. G.; Robb, M. A.; Cheeseman, J. R.; Keith, T.; Petersson, G. A.; Montgomery, J. A.; Raghavachari, K.; Al-Laham, M. A.; Zakrzewski, V. G.; Ortiz, J. V.; Foresman, J. B.; Cioslowski, J.; Stefanov, B. B.; Nanayakkara, A.; Challacombe, M.; Peng, C. Y.; Ayala, P. Y.; Chen, W.; Wong, M. W.; Andres, J. L.; Replogle, E. S.; Gomperts, R.; Martin, R. L.; Fox, D. J.; Binkley, J. S.; Defrees, D. J.; Baker, J.; Stewart, J. P.; Head-Gordon, M.; Gonzalez, C., Pople, J. A. *Gaussian 94, Revision D.4;* Gaussian, Inc.: Pittsburgh, PA, 1995.

(24) Schaftenaar, G.; Noordik, J. H. *J. Comput.-Aided Mol. Des*. **2000**, *14*, 123.

(25) The optimization of the 2a geometry yielded two CASSCF(4, 6) structures, both of them having mostly (1, 2)(1, 2) configuration. The higher-energy structure, with Ecas = −193.867624, has a CAS coefficient of 0.999, indicating that it is completely dominated by the (1, 2)(1, 2) configuration. This structure has three imaginary frequencies. The C−C bond-length and the C−C−C bending angle are 1.318 Å and 179.634°, respectively. The lower energy structure, with E_{cas} = − 193.888821 hartree, has a CAS coefficient of 0.982. In this case the main (1, 2)(1, 2) configuration is mixed with the doubly-excited (1, 3)(1, 3) configuration. The lower energy structure has four imaginary frequencies. The C−C bond-length and the C−C−C bending angle are 1.329 Å and 179.690°, respectively. In this structure the symmetries of the active space orbitals changed from (A″A″A′A′A′A′) to (A″A″A″A′A′A′). The closeness of the two structures suggests the existence of an avoided curve-crossing or of a conical intersection near the **2a** conformation.

(26) The central C=C=C carbon atom defines the origin of XY*Z* axis. The C=C=C group is located along the *Z* axis, the *X* axis is contained in the frozen plane defined by CH_3–C−H group and the *Y* axis is orthogonal to this plane.

(27) In the ground state, the distance between the two carbons belonging to the two methyl groups in the syn configuration is 4.32 Å. The smallest distance between two hydrogens belonging to the two methyls is 3.06 Å. These distances are well outside the sum of the van der Waals radii of two carbon atoms, which is 3.40 Å and that of two hydrogen atoms which is 2.40 Å.

(28) On the basis of previous DFT calculations for the nonsubstituted allene, where a first-excited-state minimum in the planar-linear configuration was found, we have used the DFT method to optimize the planar geometries of 1,3-dimethylallene. Since the DFT methods is strictly applicable to ground closed-shell configurations, the use of DFT for excited-state calculations might appear questionable. However, in our case, the excited-state geometries have closed shell electronic states, for which DFT is applicable. Using DFT in conjunction with the B3LYP method with a smaller basis set [6-31+G(d, p)] yielded a *nonplanar* minimum energy geometry of the $C_i$symmetry, with the two C−H hydrogen atoms oriented out-of-plane. This finding was confirmed by a preliminary CASSCF optimization, yielding a critical point at a nonplanar conformation.